Prolyl hydroxylase-dependent modulation of eukaryotic elongation factor 2 activity and protein translation in acute hypoxia*

Antonio Romero-Ruiz[1,$], Lucía Bautista[1,$], Virginia Navarro[2], Antonio Heras-Garvín[1], Rosana March-Díaz[1], Antonio Castellano[1], Raquel Gómez-Díaz[1], María J. Castro[1], Edurne Berra[2], José López-Barneo[1] and Alberto Pascual[1]

[1]Instituto de Biomedicina de Sevilla, Hospital Universitario Virgen del Rocío/CSIC/Universidad de Sevilla, 41013 Seville, Spain.

[2]Centro de Investigación Cooperativa en Biociencias, CIC bioGUNE, Parque Tecnológico de Bizkaia, 48160 Derio, Spain

*Running title: PHD2 activity and translational arrest in hypoxia

[$]These two authors contributed equally to this work

To whom correspondece should be addressed: Alberto Pascual or José López-Barneo, Instituto de Biomedicina de Sevilla, Hospital Universitario Virgen del Rocío.,Av. Manuel Siurot s/n, 41013 Seville, Spain, Tel.: +34955923049; Fax.: +34955923101; E-mail: apascual-ibis@us.es or lbarneo@us.es

Keywords: hypoxia; protein synthesis; translational arrest; elongation factor 2 phosphorylation; prolyl hydroxylases

Background: Translational arrest is a classical cellular response to hypoxia whose underlying mechanisms are unknown.
Results: Inhibitory phosphorylation of eukaryotic elongation factor 2 by acute hypoxia depends on oxygen-sensitive prolyl hydroxylases (PHDs).
Conclusion: Elongation phase of protein synthesis is regulated by PHDs.
Significance: This work unravels a novel cellular process controlled by PHDs, potential pharmacological targets in several human diseases.

SUMMARY

Early adaptive responses to hypoxia are essential for cell survival, but their nature and underlying mechanisms are poorly known. We have studied the post-transcriptional changes in mammalian cells' proteome elicited by acute hypoxia and found that phosphorylation of eukaryotic elongation factor 2 (eEF2), a ribosomal translocase whose phosphorylation inhibits protein synthesis, is under precise and reversible control of O_2 tension. Upon exposure to hypoxia, phosphorylation of eEF2 at Thr[56] occurs rapidly (< 15 min) and results in modest translational arrest, a fundamental homeostatic response to hypoxia that spares ATP and thus facilitates cell survival. Acute inhibitory eEF2 phosphorylation occurs without ATP depletion or AMP kinase activation. Furthermore, eEF2 phosphorylation is mimicked by prolyl hydroxylases (PHDs) inhibition with dimethyloxalylglycine (DMOG) or by selective PHD2 siRNA-silencing, but is independent of hypoxia inducible factor α stabilization. Moreover, over-expression of PHD2 blocks hypoxic accumulation of phosphorylated eEF2. Therefore, our findings suggest that eEF2 phosphorylation status, and as a consequence translational rate, is controlled by PHD2 activity. They unravel a novel pathway for cell adaptation to hypoxia that could have pathophysiologic relevance in tissue ischemia and cancer.

Cell adaptation to reduced oxygen availability to maintain ATP levels is a major physiologic challenge since O_2 deprivation,

even transient, can produce irreversible damage. Cellular responses to hypoxia comprise transcriptional and non-transcriptional mechanisms whose nature is as yet only partially known (1-3). Transcriptional adaptation to low O_2 tension mainly depends on hypoxia inducible transcription factors (HIFs), master regulators of a broad cohort of genes whose expression decreases the cellular O_2 demand and increases O_2 supply (3). Cellular levels of HIFα are inversely correlated with the activity of prolyl hydroxylases (PHDs), O_2-sensing and Fe^{2+}-dependent enzymes that hydroxylate specific proline residues in HIFα using O_2 as co-substrate, thus allowing HIFα ubiquitination and proteasomal degradation (4,5).

In contrast with the relatively well-characterized PHD-HIF pathway, the transcription-independent hypoxic adaptive mechanisms are poorly known. Nevertheless, they are essential for cell survival during the first minutes of hypoxia, before functional expression of the O_2-regulated genes can take place (2,6). Global inhibition of protein synthesis ("translational arrest") has been classically recognized as a fundamental adaptation to hypoxia, since mRNA translation is an energy-costly process that consumes up to 70% of the ATP synthesized by the cells. Hence, any small adjustment on translation rate can spare sufficient ATP as to immediately attend functions critical for cell survival (7-10). Several kinases regulated during cell energy starvation, in particular the mammalian target of Rapamycin (mTOR), the endoplasmic reticulum kinase (PERK), and AMP-activated protein kinase (AMPK), have been suggested to contribute to HIF-independent inhibition of protein translation under low O_2 conditions (7,9,11-13). These phosphorylation/ dephosphorylation cascades regulate protein synthesis by precisely modulating the activity of ribosomal initiation and elongation factors (eEF) (10,14). In this regard, elongation factor 2 (eEF2), a translocase necessary for the movement of the mRNA along the ribosome, is particularly important as, in conjunction with aminoacylation, it uses most of the ATP required for protein synthesis (15). eEF2 is inhibited by phosphorylation at Thr^{56} by eEF2 kinase (eEF2K), (16,17), which in turn is activated by AMPK (18).

Using a proteomic approach designed to detect early adaptive changes during short (5-30 min) exposure to hypoxia, we have identified several proteins acutely regulated by O_2 availability. Among these proteins eEF2 was also modulated by DMOG, an inhibitor of the O_2 sensing PHDs. Herein, we describe that eEF2 activity is rapidly and reversibly regulated by O_2 tension in a PHD2-dependent manner. This phenomenon is unrelated with HIF stabilization and it occurs prior to AMPK activation. These observations, that unveil unexpected actions of the O_2-sensing PHD2, could have profound implications for the pathophysiology and pharmacology of cell adaptation to hypoxia.

EXPERIMENTAL PROCEDURES

Cell culture and hypoxic treatments–PC12, Mlp9, HeLa, and HuH7 cells were cultured in DMEM (Bio-Whittaker) supplemented with 10% FBS (Gibco), 100 U/mL penicillin, 100 U/mL streptomycin and 2 mM L-glutamine (Bio-Whittaker). Cardiac ventricular myocytes were prepared from 1- to 3-day-old animals and cultured as described by (19). Hepatocytes were isolated from male Wistar rats by collagenase (Invitrogen) perfusion as described previously (44). U2OS Tet-ON and U2OS Tet-ON/pUHD-Flag-PHD2 cells were cultured in DMEM supplemented with 10% tetracycline-free FBS (Clontech/Takara), 100 U/mL penicillin, 100 U/mL streptomycin, and 5 μg/mL Blasticidine S (Invitrogen). 200 μg/mL Hygromycin-B (Roche) was used in U2OS Flag-PHD2 cultures. Cells were maintained under water-saturated atmosphere of 5% CO_2-95% air. DMOG (Biomol International L.P.) was used at a final concentration of 1 mM, NaF (SIGMA) was used at 25 mM, and AICAR (SIGMA) at 1 mM. Okadaic acid (Calbiochem), Sanguinarine (SIGMA) were used at the concentrations specified.

Hypoxic conditions (1% O_2, 94% N_2, and 5% CO_2) were achieved in a humidified variable aerobic workstation (Invivo$_2$ 300; Ruskin). In all experiments, cells were plated at 30%–50% confluence to prevent the development of anaerobic conditions at 1% O_2.

Before experimentation, media were pre-equilibrated overnight to the experimental oxygen level.

Protein Analysis–Sample preparation, labeling and analysis by 2D-DIGE. Sup100 protein extracts from PC12 cells were prepared and labeled as described (20). 150 µg of labeled protein, containing three equal amount extracts (Normoxic, Hypoxic or DMOG treated, and the internal standard) were used for 2D-DIGE. Electrophoretic conditions, quantitative analysis of differences, and preparative gels were performed as described (20). Four biological replicates were used in all the experiments.

eEF2 purification from rat liver. Rat liver were homogenized and eEF2 purified as described by (21) using an ÄKTA purifier (GE Healthcare).

Western blot, protein synthesis measurements, and MALDI-MS/MS analysis are described in the Supplemental methods accompanying this paper.

RNA interference–Transfections of siRNAs were carried out using Lipofectamine 2000 (Invitrogen) at a final concentration of 20 nM. Previously validated sequences of siRNAs were used (22,23). However the efficacy of the transfection in each experiment was ascertained by immunoblotting and/or RT-qPCR. Non-published siRNAs and oligonucleotides sequences can be found in Supplemental methods.

ATP Measurements–ATP levels in cell extracts were determined by ATP bioluminescence assay kit CLS II (Roche Applied Science) using GLOMAX^{TM} 96 microplate luminometer equipped with an auto-injection device (Promega).

Statistics–Data are presented as mean ± S.E.M. and were analyzed with one-way analysis of variance followed by Tukey's test. $p < 0.05$ was considered statistically significant.

RESULTS

Acute O_2-Dependent Modulation of Cell Proteome–We performed proteomic (2D-DIGE) analyses of soluble subcellular fractions (S100) (20) obtained from homogenates of PC12 cells exposed to normoxia (21% O_2) or hypoxia (1% O_2) for 15 to 30 min. A 2D map of the S100 fraction is shown in Fig. 1*a* with spots whose relative amounts increased (red), decreased (green), or were unchanged (yellow) in hypoxia. Among the 2598 spots detected, 24 were identified in all the experimental replicates and changed their relative amount in hypoxia versus normoxia (> 1.5-fold and $p < 0.05$. See Supplemental Table I). In 2D gels, eEF2 appeared in a strip of spots that could correspond to additive modifications of the protein (Fig. 1A, white rectangle), hence we extended our analysis to additional neighboring spots. These modifications are probably due to different diphthamide content in eEF2. Among the 7 spots studied (Fig. 1B, top), 5 were identified as eEF2 by MALDI-MS(/MS) (asterisks), and all were recognized by an anti-eEF2 antibody (Fig. 1B, middle). Accordingly, eEF2 purified from rat liver and separated in a 2D electrophoresis showed a similar distribution (Fig. 1B, bottom). These results revealed that eEF2 is modified by short exposure to hypoxia, thus suggesting that it could be a mediator of the early adaptive mechanisms triggered by low O_2 tension.

It is known that eEF2 activity is inhibited by phosphorylation at Thr^{56} through a specific eEF2 kinase (16,17). Therefore, we tested in several cell types whether the changes in eEF2 observed in the 2D-DIGE analyses correlated with modifications in eEF2 Thr^{56} phosphorylation status using specific P-Thr^{56} antibodies. Hypoxia (1% O_2) produced a marked increase in eEF2 phosphorylation that was detectable 15 min after exposure of cells to low O_2 tension. Total amount of eEF2 was unchanged by exposure to hypoxia (Fig. 1C-E; SFig. 1A, B).

Inhibitory eEF2 Phosphorylation in Acute Hypoxia Occurs Before ATP Depletion and AMPK Activation–As mentioned before, several kinases modulated by energy starvation are also regulated during sustained hypoxic conditions (7,9,12,13,18). AMPK, activated by phosphorylation at Thr^{172} by liver kinase B1 (LKB1) when the AMP/ATP ratio increases (24-27), can activate eEF2K through phosphorylation at Ser^{398} (18) and thus induce inhibitory Thr^{56} phosphorylation of eEF2 (16,17). We postulated that the fast, O_2-dependent modulation of eEF2 reported here

should occur prior to, and independently of, AMPK activation.

As expected, exposure of hepatocytes to 1% O_2 revealed a clear increase in eEF2-Thr^{56} phosphorylation detectable as soon as 5 min after O_2 deprivation, without any increase in the levels of active AMPK (phosphorylated at Thr^{172}). In contrast, cells treated with 5-aminoimidazole-4-carboxiamide riboside (AICAR), an AMPK activator used as a control (28), showed strong activation of AMPK (Fig. 2A). Short-lasting exposure to hypoxia also resulted in an increase of eEF2-P-Thr^{56} and decrease of AMPK-P-Thr^{172} levels in other cell types analyzed (Fig. 2B). Interestingly, the amount of active AMPK during hypoxic exposures lasting up to 4 h remained even lower than the value in normoxia (Fig. 2A, B). In fair agreement with these data, cellular ATP concentration did not change (or even increased) after 15 or 60 min in hypoxia (1% O_2) (Fig. 2C). The activity of eEF2K is inhibited by phosphorylation at Ser^{366}, a process regulated by p90^{RSK}/p70S6 kinases (18). Short hypoxia did not produce any changes in the cellular levels of eEF2K-P-Ser^{366} (Figure 1C). Hypoxia treatment did not alter the total levels of eEF2, eEF2K, or AMPK (Fig. 1C, 2B).

Hypoxia and Prolyl Hydroxylase 2 Inhibition Increase eEF2 Phosphorylation in a HIF-Independent Manner–To test whether some of the identified proteins modified by hypoxia could be under the control of the O_2 sensing PHDs, cells were exposed to dimethyloxalylglycine (DMOG), a competitive inhibitor of 2-oxoglutarate-dependent dioxygenases, including PHDs (4,29). Control (untreated) and 15 min DMOG-treated cells were processed by 2D-DIGE and a representative gel of the S100 fraction is shown in Fig. 3A, with proteins whose relative amounts increased (green), decreased (red), or were unchanged (yellow) after DMOG treatment. Only spot 1, identified by mass fingerprinting analysis as eEF2, changed both in hypoxia (see Fig. 1A) and after DMOG treatment (Fig. 3A). As hypoxia, DMOG treatment also elicited in several cell types a similar P-Thr^{56} eEF2 accumulation although with a slower time course (Fig. 3B-D*;* SFig. 1B). DMOG-triggered accumulation of either HIF-1α or HIF-2α, used as controls (Fig. 3C, D), was also delayed compared to hypoxia, thus possibly reflecting DMOG cellular uptake and metabolization to the active N-oxalylglycine inhibitor.

As transformed cell lines normally show some resistance to hypoxic translational arrest (30), we estimated if the increase in phosphorylation of eEF2 by short hypoxia or DMOG induced a concomitant decrease in protein translation in primary cultured hepatocytes (Fig. 3E). As expected, hypoxic and DMOG treatments resulted in a significant decrease in protein synthesis rate as determined by ^{35}S-met incorporation assay (Fig. 3F).

Hypoxia and DMOG rapidly inhibit PHDs, therefore the involvement of these enzymes in modulation of protein synthesis was studied using cells incubated with siRNA specific to each PHD (22). We observed a selective increase of eEF2-P-Thr^{56} after PHD2 silencing, and no effect after inhibition of either PHD1 or PHD3 (Fig. 4A). The effectiveness of the siRNA treatment on PHDs mRNA was confirmed by qRT-PCR (Supplemental Table II). PHD2 silencing was also demonstrated by selective stabilization of HIF-1α (Fig. 4A). PHD down-regulation studied in several cell types always correlated with hyperphosphorylation of eEF2 at Thr^{56} (SFig. 2A).

To further prove the direct involvement of PHD2 in the regulation of eEF2 by acute hypoxia we have used a cell line (U2OS) where PHD2 expression is conditionally induced by doxycycline (Norma Masson and Peter Ratcliffe, unpublished material). Overexpression of PHD2 is known to inhibit stabilization of HIF-1 and 2α in hypoxia (23,31), hence we tested whether PHD2 overexpression also prevents eEF2 phosphorylation by acute hypoxia. After 4 h in doxycycline, expression of PHD2 was observed in U2OS cells (Fig. 4B) and was correlated with a clear decrease in the amount of eEF2 phosphorylated after 30 min of hypoxic treatment (Fig. 4B; see quantification in Fig. 4C, $p = 0.024$). As a control, we tested that HIF-1α stabilization by hypoxia was also partially prevented by PHD2 expression (Fig. 4B; see quantification in Fig. 4C, $p = 0.044$).

Because inhibition of PHD2 by hypoxia, DMOG, or siRNA leads to HIF-α accumulation, we investigated whether HIF might regulate eEF2 phosphorylation at Thr^{56}. Although expression of either HIF-1α or HIF-2α in hypoxia was clearly abolished using specific siRNAs, eEF2 phosphorylation was unaltered (Fig. 4D, upper panel). Hypoxia-dependent eEF2 phosphorylation was observed even though HIF-1α and HIF-2α were simultaneously silenced to prevent possible compensatory effects of any of the isoforms (Fig. 4D, bottom panel). The dispensability of HIFα for the hypoxic/DMOG-induced eEF2 phosphorylation was further confirmed by using a genetically modified embryonic stem cell line lacking HIF-1α (32), (SFig. 2B).

eEF2 phosphorylation by hypoxia is reversible and strongly controlled by phosphatases activity–Accumulation of phosphorylated eEF2 under hypoxia was rapidly (< 15 min) reversed upon reoxygenation, independently of the duration of the hypoxic treatment (Fig. 5A), thus supporting the notion that O_2-dependent eEF2 phosphorylation is indeed a tightly regulated process. Furthermore, inhibition of Ser/Thr phosphatases with sodium fluoride (NaF) produced a marked increase in the amount of eEF2-P-Thr^{56}, which was not further modified by subsequent exposure to hypoxia. In contrast, phosphorylation of eEF2K at Ser^{366}, used as control for phosphatase activity, was unchanged. Hence, eEF2-P-Thr^{56} appears to be highly susceptible to the action of phosphatases (Fig. 5B). To identify the phosphatase acting on eEF2 we have used inhibitors more specific than NaF. It has been described that eEF2 can be dephosphorylated by PP2A and PP2C (33,34). Hence, we tested specific inhibitors for each phosphatase and analyzed where they reproduce the fast changes in the level of phosphorylation of eEF2 observed under hypoxia. Short okadaic acid treatment (a PP2A inhibitor) produced a strong accumulation of eEF2 (Figure 5C, left panel), but sanguinarine (a PP2C inhibitor) did not affect the phosphorylation status of eEF2 (Figure 5C, right panel). These results suggest that PP2A control the phosphorylation status of eEF2 under normoxia.

DISCUSSION

In this report we describe selective post-transcriptional adaptive changes in mammalian cells' proteome elicited by acute hypoxia. This study focuses on eEF2, a translocase necessary for protein synthesis, although we have identified two other proteins (arginyl aminopeptidase and protease inhibitor Serpinb6) also altered by lowering O_2 tension (See Supplemental Table I). We show that hypoxic inhibitory eEF2 phosphorylation is independent of AMPK activity and is mimicked by DMOG treatment, thus suggesting the notion that eEF2 activity and protein synthesis are modulated by PHDs.

Translational arrest is a classically studied cellular response to anoxia or long-term hypoxia (for a review see 14). It has also been reported that short (2 h) exposure to moderate hypoxia (0.2-2% O_2) can lead to a modest but reproducible decrease in translation efficiency (35), an effect that is better observed with longer (> 24 h) treatments (12,13,36,37). We show here that acute (5-15 min) hypoxia (1% O_2) or DMOG treatment leads to changes on eEF2 migration pattern as a consequence of increased protein phosphorylation at Thr^{56}. It is well established that phosphorylation of eEF2 at Thr^{56} decreases the rate of protein elongation (17,38), a mechanism that can contribute to mRNA translation inhibition by hypoxia and DMOG observed in primary cultured cardiomyocytes (Fig. 3F). Similar results have been reported using tumor/immortalized cell lines (12,13) but longer periods, more severe hypoxia, or even concomitant serum withdrawal were required to observe a decrease in protein synthesis in these cellular models that are normally resistant to mRNA translation inhibition by hypoxia (30).

The activation of the AMPK/eEF2K/eEF2 pathway to arrest protein translation under long-term hypoxia or ischemia has been elegantly demonstrated in previous reports (12,13). However, the inhibition of eEF2 activity observed under acute hypoxia described here is independent of this pathway. Indeed, we have shown that short-term hypoxia even decreases AMPK activity in all cells tested (Fig. 2A, B). In agreement with this data,

cellular ATP levels were preserved or increased upon acute exposure to acute hypoxia (Fig. 2C) (see also 13,39). The existence of complementary PHD2- and AMPK-dependent eEF2 modulator pathways set in motion depending on O_2 availability is advantageous because it offers a broader adaptive repertoire to ensure ATP homeostasis.

As DMOG inhibits a broad family (> 50 members) of 2-oxoglutarate-dependent dioxygenases (4,29), we performed siRNA analyses to identify the PHDs involved in eEF2 regulation. We have found that selective inhibition of PHD2 in several cell lines leads to a sustained eEF2 phosphorylation at Thr^{56}, thus confirming that protein synthesis is modulated by the activity of the O_2 sensor PHD2 (Fig. 4A and SFig. 2B). To achieve a strong silencing of PHD2, cells were treated with siRNAs for 72 h, inducing several HIF-regulated pathways that could, indirectly, lead to phosphorylation of eEF2. However, over-expression of PHD2 for 4 h produces a strong inhibition of the hypoxia dependent phosphorylation of eEF2 (Fig. 4B, C), an effect that has been also shown for hypoxia-induced HIF stabilization (23,31). Altogether, these data suggest a control of PHD2 over the elongation phase of protein translation. PHD2-dependent regulation of translation is independent of HIF-α activity and takes place few minutes after PHDs inhibition (Fig. 4C and SFig. 2B). Sequence analyses reveal the presence in eEF2 of three motifs consisting of a proline preceded by two neighboring leucines (LXLXP), resembling the hydroxylation consensus motifs (LXXLAP) existing in the O_2-dependent degradation domain (ODDD) of HIF-α (4,5). However, additional work will be required to determine if PHD2 regulates eEF2 by direct hydroxylation of these residues or, alternatively, modulates the activity of other proteins, including eEF2K or any subunit of the cellular phosphatases.

O_2 influx to tissues can be a fluctuating condition (40), thus the mechanisms regulating hypoxic responses must be reversible and easily adjustable to oxygen availability. Interestingly, phosphorylation of eEF2 is tightly regulated by the activity of specific kinases and phosphatases (33,34,36). We show here that phosphorylation of eEF2 at Thr^{56} by hypoxia is quickly reversed upon returning to normoxia (Fig. 5A). Short exposure (10 min) of cells to a Ser/Thr phosphatase inhibitor lead to marked accumulation of phosphorylated eEF2, indicating a high basal activity of phosphatases acting on eEF2 (Fig. 5B). Our pharmacological studies revealed that acute inhibition of PP2A activity leads to a similar accumulation of phosphorylated eEF2 (Fig. 5C), suggesting a role of this protein in the regulation of protein synthesis by acute hypoxia. The tightly regulation and the fast reversibility of eEF2 phosphorylation/dephosphorylation status make this protein an ideal candidate to control protein synthesis rate in response to variable conditions of tissue O_2 availability.

In conclusion, we propose a novel mechanism that helps explain acute translation arrest in hypoxia, which is AMPK- and HIF-independent, and relies on PHD2-mediated regulation of eEF2 activity (see scheme in Fig. 6). However, complete understanding of the mechanism whereby PHD2 regulates eEF2 phosphorylation must await further investigation. Besides its obvious interest in the biology of hypoxia and hypoxia/reperfusion, the PHD2-eEF2 pathway could open new perspectives relevant for the pharmacology of tissue ischemia and cancer.

REFERENCES

1. Kaelin, W. G., Jr., and Ratcliffe, P. J. (2008) *Mol. Cell.* **30**, 393-402
2. Lopez-Barneo, J., Pardal, R., and Ortega-Saenz, P. (2001) *Annu. Rev. Physiol.* **63**, 259-287
3. Semenza, G. L. (2009) *Physiology (Bethesda)* **24**, 97-106
4. Epstein, A. C., Gleadle, J. M., McNeill, L. A., Hewitson, K. S., O'Rourke, J., Mole, D. R., Mukherji, M., Metzen, E., Wilson, M. I., Dhanda, A., Tian, Y. M., Masson, N., Hamilton, D. L., Jaakkola, P., Barstead, R., Hodgkin, J., Maxwell, P. H., Pugh, C. W., Schofield, C. J., and Ratcliffe, P. J. (2001) *Cell* **107**, 43-54

5. Masson, N., Willam, C., Maxwell, P. H., Pugh, C. W., and Ratcliffe, P. J. (2001) *EMBO J.* **20**, 5197-5206
6. Weir, E. K., Lopez-Barneo, J., Buckler, K. J., and Archer, S. L. (2005) *N. Engl. J. Med.* **353**, 2042-2055
7. Arsham, A. M., Howell, J. J., and Simon, M. C. (2003) *J. Biol. Chem.* **278**, 29655-29660
8. Hochachka, P. W., Buck, L. T., Doll, C. J., and Land, S. C. (1996) *Proc. Natl. Acad. Sci.* **93**, 9493-9498
9. Koumenis, C., Naczki, C., Koritzinsky, M., Rastani, S., Diehl, A., Sonenberg, N., Koromilas, A., and Wouters, B. G. (2002) *Mol. Cell. Biol.* **22**, 7405-7416
10. Wouters, B. G., van den Beucken, T., Magagnin, M. G., Koritzinsky, M., Fels, D., and Koumenis, C. (2005) *Semin. Cell. Dev. Biol.* **16**, 487-501
11. Browne, G. J., and Proud, C. G. (2004) *Mol. Cell. Biol.* **24**, 2986-2997
12. Connolly, E., Braunstein, S., Formenti, S., and Schneider, R. J. (2006) *Mol. Cell. Biol.* **26**, 3955-3965
13. Liu, L., Cash, T. P., Jones, R. G., Keith, B., Thompson, C. B., and Simon, M. C. (2006) *Mol. Cell.* **21**, 521-531
14. Koritzinsky, M., and Wouters, B. G. (2007) *Methods Enzymol.* **435**, 247-273
15. Proud, C. G. (2007) *Biochem. J.* **403**, 217-234
16. Nairn, A. C., and Palfrey, H. C. (1987) *J. Biol. Chem.* **262**, 17299-17303
17. Ryazanov, A. G., Shestakova, E. A., and Natapov, P. G. (1988) *Nature* **334**, 170-173
18. Browne, G. J., Finn, S. G., and Proud, C. G. (2004) *J. Biol. Chem.* **279**, 12220-12231
19. Akao, M., Ohler, A., O'Rourke, B., and Marban, E. (2001) *Circ. Res.* **88**, 1267-1275
20. Pascual, A., Romero-Ruiz, A., and Lopez-Barneo, J. (2009) *Proteomics* **9**, 2946-2954
21. Horman, S., Browne, G., Krause, U., Patel, J., Vertommen, D., Bertrand, L., Lavoinne, A., Hue, L., Proud, C., and Rider, M. (2002) *Curr. Biol.* **12**, 1419-1423
22. Berra, E., Benizri, E., Ginouves, A., Volmat, V., Roux, D., and Pouyssegur, J. (2003) *EMBO J.* **22**, 4082-4090
23. Ginouves, A., Ilc, K., Macias, N., Pouyssegur, J., and Berra, E. (2008) *Proc. Natl. Acad. Sci.* **105**, 4745-4750
24. Hardie, D. G., Scott, J. W., Pan, D. A., and Hudson, E. R. (2003) *FEBS Lett.* **546**, 113-120
25. Hawley, S. A., Davison, M., Woods, A., Davies, S. P., Beri, R. K., Carling, D., and Hardie, D. G. (1996) *J. Biol. Chem.* **271**, 27879-27887
26. Lizcano, J. M., Goransson, O., Toth, R., Deak, M., Morrice, N. A., Boudeau, J., Hawley, S. A., Udd, L., Makela, T. P., Hardie, D. G., and Alessi, D. R. (2004) *EMBO J.* **23**, 833-843
27. Shaw, R. J., Kosmatka, M., Bardeesy, N., Hurley, R. L., Witters, L. A., DePinho, R. A., and Cantley, L. C. (2004) *Proc. Natl. Acad. Sci.* **101**, 3329-3335
28. Corton, J. M., Gillespie, J. G., Hawley, S. A., and Hardie, D. G. (1995) *Eur. J. Biochem.* **229**, 558-565
29. Jaakkola, P., Mole, D. R., Tian, Y. M., Wilson, M. I., Gielbert, J., Gaskell, S. J., Kriegsheim, A., Hebestreit, H. F., Mukherji, M., Schofield, C. J., Maxwell, P. H., Pugh, C. W., and Ratcliffe, P. J. (2001) *Science* **292**, 468-472
30. Hockel, M., and Vaupel, P. (2001) *J. Natl. Cancer Inst.* **93**, 266-276
31. Takeda, K., and Fong, G. H. (2007) *Hypertension* **49**, 178-184
32. Carmeliet, P., Dor, Y., Herbert, J. M., Fukumura, D., Brusselmans, K., Dewerchin, M., Neeman, M., Bono, F., Abramovitch, R., Maxwell, P., Koch, C. J., Ratcliffe, P., Moons, L., Jain, R. K., Collen, D., and Keshert, E. (1998) *Nature* **394**, 485-490
33. Redpath, N. T., and Proud, C. G. (1990) *Biochem. J.* **272**, 175-180
34. Redpath, N. T., and Proud, C. G. (1991) *Biochim. Biophys. Acta* **1093**, 36-41
35. Koritzinsky, M., Rouschop, K. M., van den Beucken, T., Magagnin, M. G., Savelkouls, K., Lambin, P., and Wouters, B. G. (2007) *Radiother. Oncol.* **83**, 353-361
36. Lang, K. J., Kappel, A., and Goodall, G. J. (2002) *Mol. Biol. Cell* **13**, 1792-1801

37. Thomas, J. D., and Johannes, G. J. (2007) *RNA* **13**, 1116-1131
38. Redpath, N. T., Price, N. T., Severinov, K. V., and Proud, C. G. (1993) *Eur. J. Biochem.* **213**, 689-699
39. Lefebvre, V. H., Van Steenbrugge, M., Beckers, V., Roberfroid, M., and Buc-Calderon, P. (1993) *Arch. Biochem. Biophys.* **304**, 322-331
40. Bristow, R. G., and Hill, R. P. (2008) *Nat. Rev. Cancer* **8**, 180-192

Acknowledgments–Research was supported by the Spanish Ministry of Science and Health, the Marcelino Botin Foundation, and the Andalusian Government. We thank Peter Ratcliffe and Norma Masson for providing unpublished U2OS cell lines. A.R.-R. is a fellow of the Spanish "Sara Borrell" program. We thank Drs M. L. Martínez-Chantar and M. Varela (CIC bioGUNE) for kindly providing with the hepatocytes primary cultures.

FOOTNOTES

[1]The abbreviations used are: DMOG, dimethyloxalylglycine; PHDs, prolyl hydroxylases; HIFs, hypoxia inducible transcription factors; mTOR, mammalian target of Rapamycin; PERK, endoplasmic reticulum kinase; LKB1, liver kinase B1; AMPK, AMP-activated protein kinase; eEF, eukaryotic elongation factors; eEF2K, eEF2 kinase; AICAR, 5-aminoimidazole-4-carboxiamide riboside; NaF, sodium fluoride

FIGURE LEGENDS

FIGURE 1. Acute inhibitory eEF2 phosphorylation (Thr^{56}) is induced by hypoxia. A. Representative 2D gel. Extracts from normoxic (21% O_2, green) or hypoxic (1% O_2, 15 min; red) PC12 cells migrated in the same gel. Numbered spots correspond to the spots listed in Supplemental Table I. The internal standard extract is not shown in the image. B. Same spots as those included inside the white rectangle in "*a*" labeled with CyDyes from a different 2D-gel (top). Five spots (asterisks) were identified as eEF2 by peptide mass fingerprinting analysis. Western blot of the marked spots using an anti-eEF2 antibody (α-eEF2, center). eEF2 purified from rat liver, separated by 2D electrophoresis and detected by Sypro staining (bottom). C. Phosphorylation of eEF2 (Thr^{56}) in HuH7 subjected to normoxia (N) or hypoxia (H: 1% O_2) for 15 to 240 min. Levels of eEF2K, eEF2k-Ser^{366}, ß-actin, HIF-1α, and 2α were analyzed in the same cell extracts. D. Quantification of eEF2-P-Thr^{56} levels in (C) (r.u.: relative units). E. Hepatocytes subjected to normoxia (N) or hypoxia (H: 1% O_2) for 15 min. Two independent experiments are shown. Total levels of eEF2 and ß-actin were analyzed by Western blot.

FIGURE 2. Inhibitory eEF2 phosphorylation in acute hypoxia is independent of AMPK activity. A. Phosphorylation of eEF2 (Thr^{56}) and AMPK (Thr^{172}) analyzed by Western blot in hepatocytes subjected to hypoxia (H) for 5-240 min or treated with the AMPK activator AICAR for 240 min as a control. B. Phosphorylation of eEF2 (Thr^{56}) and AMPK (Thr^{172}) analyzed by Western blot in PC12 (left panels) or HuH7 (right panels) cells exposed to normoxia (N) or hypoxia (H) for 5 or 15 min. Total AMPK, eEF2K, and ß-actin were used as loading controls. C. ATP levels in HeLa (left bars) and HuH7 (right bars) cell lysates exposed to normoxia (N) or hypoxia (H) for 15 or 60 min. Dashed lines represent normoxic levels; ($n = 5$; $*p < 0.05$).

FIGURE 3. Acute inhibitory eEF2 phosphorylation (Thr^{56}) induced by DMOG treatment. A. Representative 2D gel showing protein extracts from control (red) or DMOG-treated (green) cells. The encircled spot was differentially expressed after DMOG treatment and is similar to spot 1 in Fig. 1A. The rectangle represents the same area of the gel shown in Fig. 1A. B. A 2D gel region showing spots modified by hypoxia (upper panel) and DMOG (bottom panel). C. Phosphorylation

of eEF2 (Thr^{56}) in HuH7 subjected to normoxia (N) or DMOG (1 mM) for 15 to 240 min. Levels of eEF2K, eEF2K-Ser^{366}, ß-actin, HIF-1α, and 2α were analyzed in the same cell extracts. D. Quantification of eEF2-P-Thr^{56} levels in (C) (r.u.: relative units). E. Hepatocytes subjected to normoxia (N) or DMOG (1 mM) for 15 min. Two independent experiments are shown. Total levels of eEF2 and ß-actin were analyzed by Western blot. F. Protein synthesis (^{35}S-Met incorporation) in cardiomyocytes exposed to normoxia (N), DMOG, or hypoxia (H) for 4 hours. Data are represented relative to N; ($n = 5$; $*p < 0.05$).

FIGURE 4. Hypoxic eEF2 phosphorylation is regulated by PHD2 in a HIF independent manner. A. Phosphorylation of eEF2 (Thr^{56}) and levels of HIF-1α examined by Western blot 48 h after siRNA transfection. HeLa cells were transfected with either PHD siRNAs or with a non-silencing scramble siRNA (Control). Control cells were independently subjected to hypoxia (H) for 15 min. In all the experiments, sample loading was normalized with total eEF2 and ß-actin. B. Hypoxic eEF2 phosphorylation at Thr^{56} is prevented by acute PHD2 overexpression. Phosphorylation of eEF2 in control or PHD2-expressing U2OS cells (Flag-PHD2). Cells were treated with doxycycline (Dox) for 4 h when indicated (+) and subjected to normoxia (N) or hypoxia (H, 1% O_2) for 30 min. Levels of HIF-1α and Flag-PHD2 were analyzed in the same cell extracts. Total levels of eEF2 and ß-actin were also analyzed by Western blot. C. Quantification of the fold change produced in the levels of eEF2-P-Thr^{56} (black bars) and HIF-1α (gray bars) by 30 min of hypoxia in the absence (–) or the presence (+) of Dox in FLAG-PHD2 cell cultures (*, $p < 0.05$, $n = 3$). D. Hypoxic eEF2 phosphorylation at Thr^{56} is independent of HIF-α activity. HeLa cells were transfected with a scrambled siRNA (Control), siHIF-1α, siHIF-2α (upper panels), or both (bottom panels) for 24 hr, and exposed to hypoxia (H) for 0, 15, or 240 min. Levels of eEF2-P-Thr^{56}, eEF2, HIF-1α, HIF-2α, and ß-act were analyzed by Western blot.

FIGURE 5. Phosphorylation of eEF2 at Thr^{56} is dynamic. A. Levels of eEF2 phosphorylation (Thr^{56}) in HuH7 cells subjected to hypoxia (H) for 15 (upper panel) or 60 (lower panel) min and recovery after returning to normoxia for 15-240 min (Reox). B. Phosphorylation of eEF2 (Thr^{56}) and eEF2K (Ser^{366}) in HeLa cells treated with the Thr/Ser phosphatase inhibitor NaF (25 mM) for 10 min. Cells were also exposed to normoxia (N) or hypoxia (H) for 15 min. Total level of eEF2K, eEF2, and ß-actin were also analyzed by Western blot. C. Phosphorylation of eEF2 at Thr^{56} is enhanced by short okadaic acid treatment (OA, 250 nM; left panel) and not affected by treatment with sanguinarine (SA, 0.5-2.5 μM, right panel). NaF (25 mM) treatment was performed as a control.

FIGURE 6. Schematic representation of the eEF2 cycle in the ribosome (blue drawing). In normoxia (left), eEF2K/Protein Phosphatase (PP) balance is displaced to the unphosphorylated form of eEF2 (green balls) in a PHD2 dependent process. Acute hypoxia (center) inhibits PHD2 activity and leads to increased eEF2 phosphorylation (red balls), which slows down the eEF2 cycle. In sustained hypoxia or anoxic/ischemic conditions (right), AMPK is activated, which leads to stimulatory eEF2K phosphorylation (Ser^{399}), eEF2 phosphorylation, and strong inhibition of elongation rate.

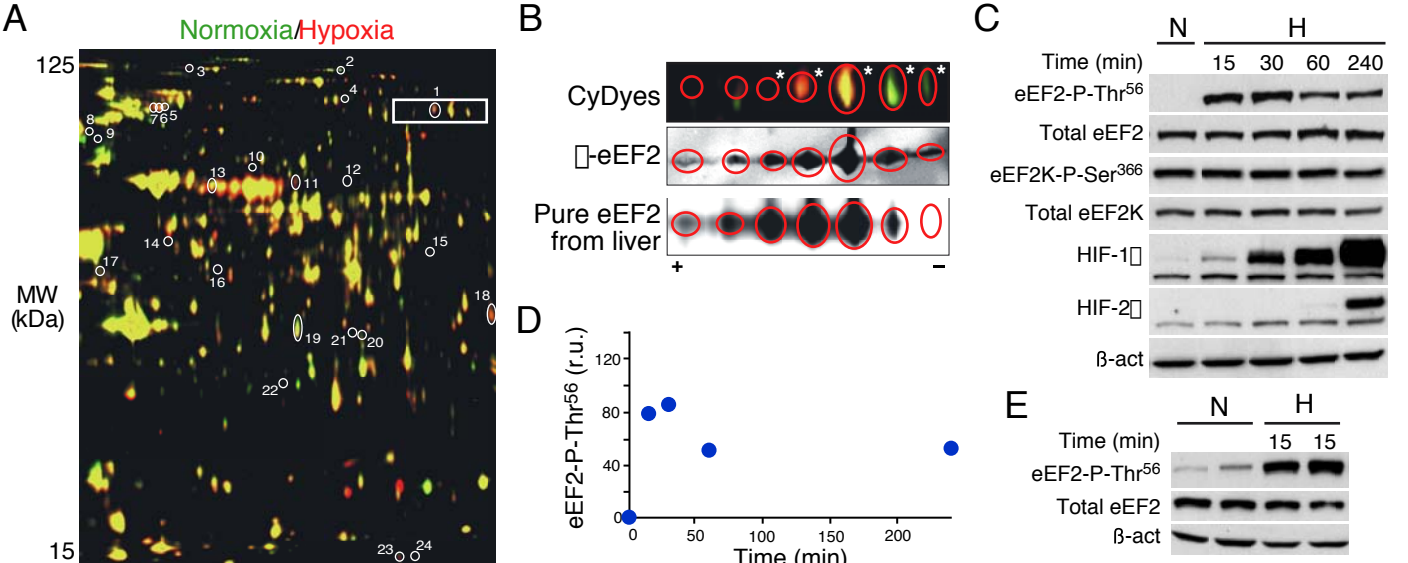

Romero-Ruiz *et al*. Figure 1

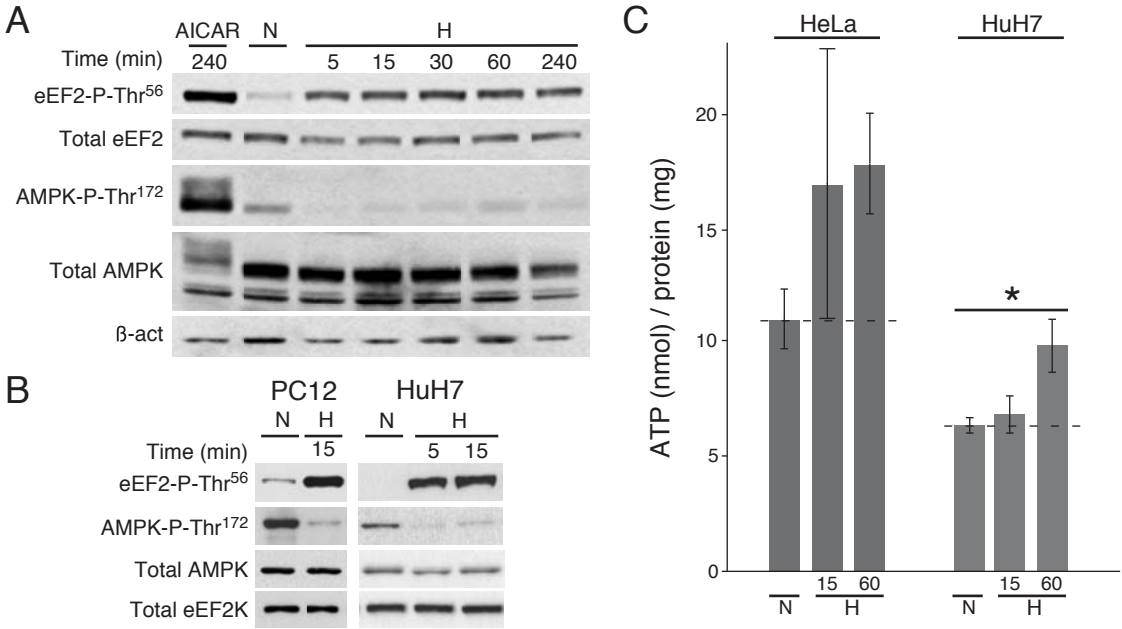

Romero-Ruiz *et al*. Figure 2

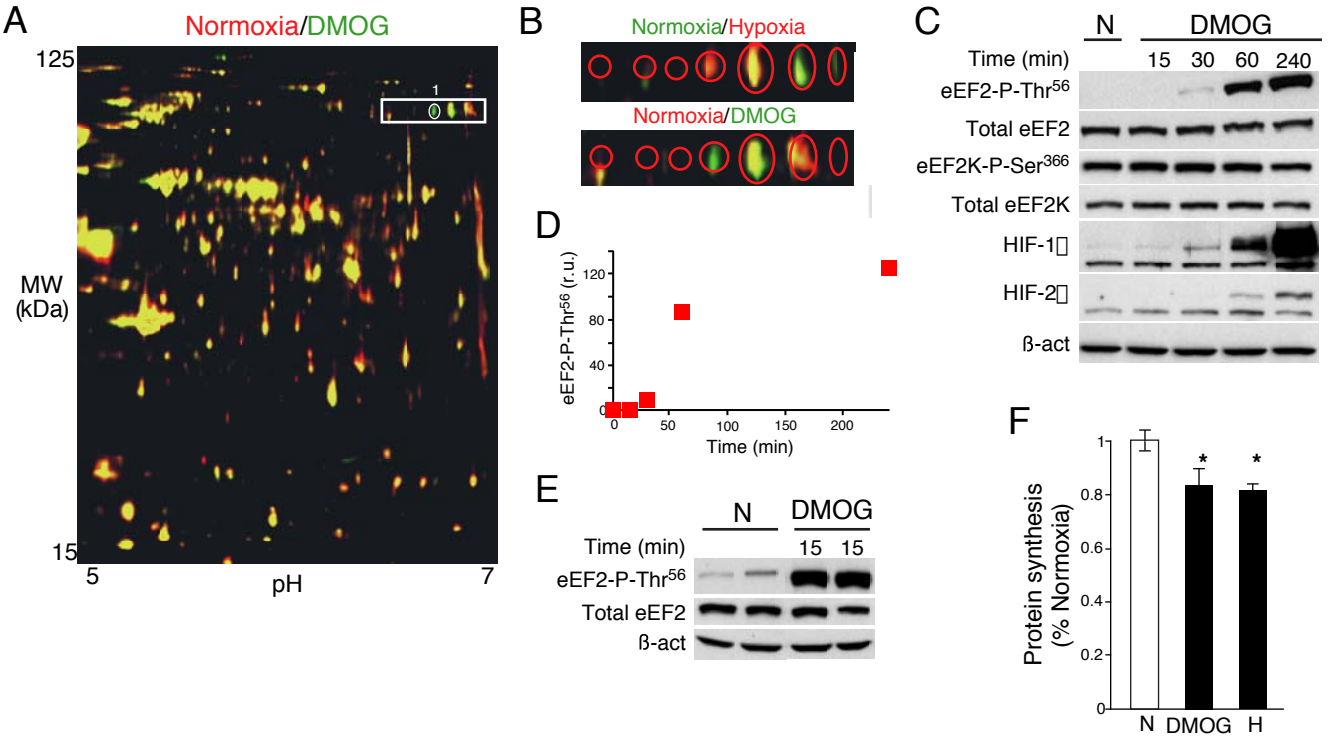

Romero-Ruiz *et al*. Figure 3

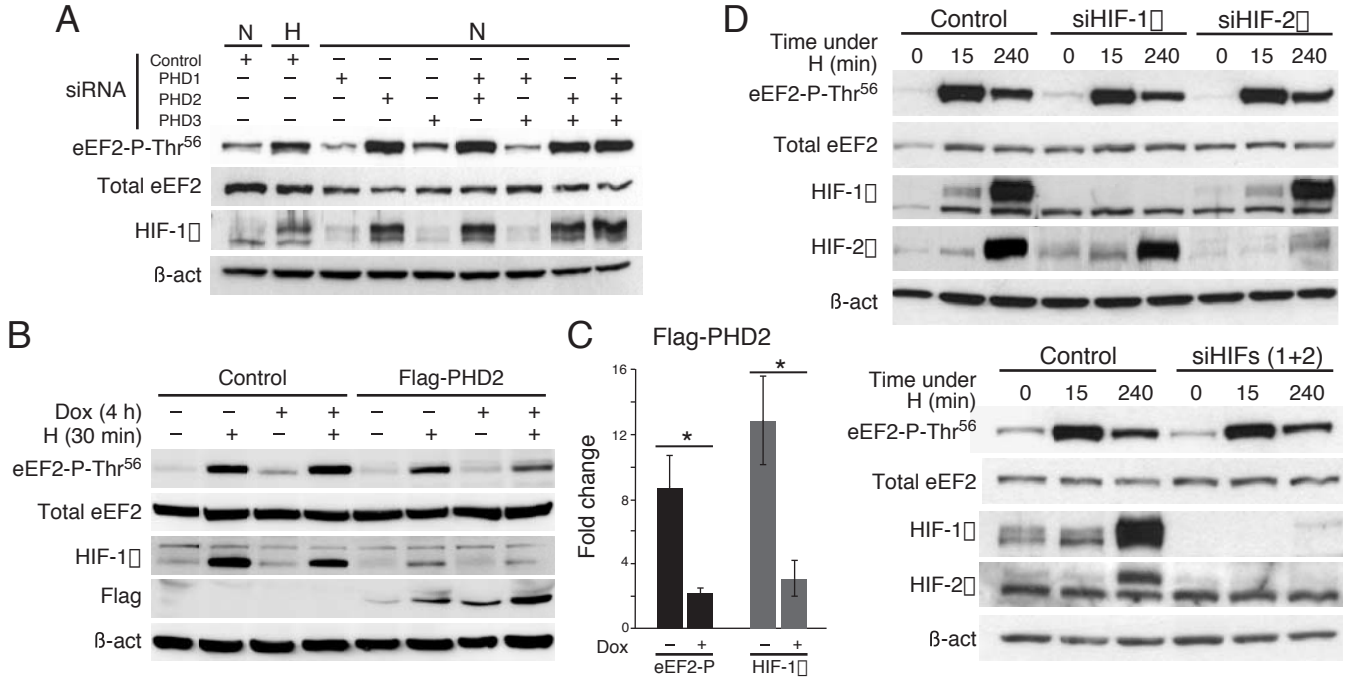

Romero-Ruiz *et al*. Figure 4

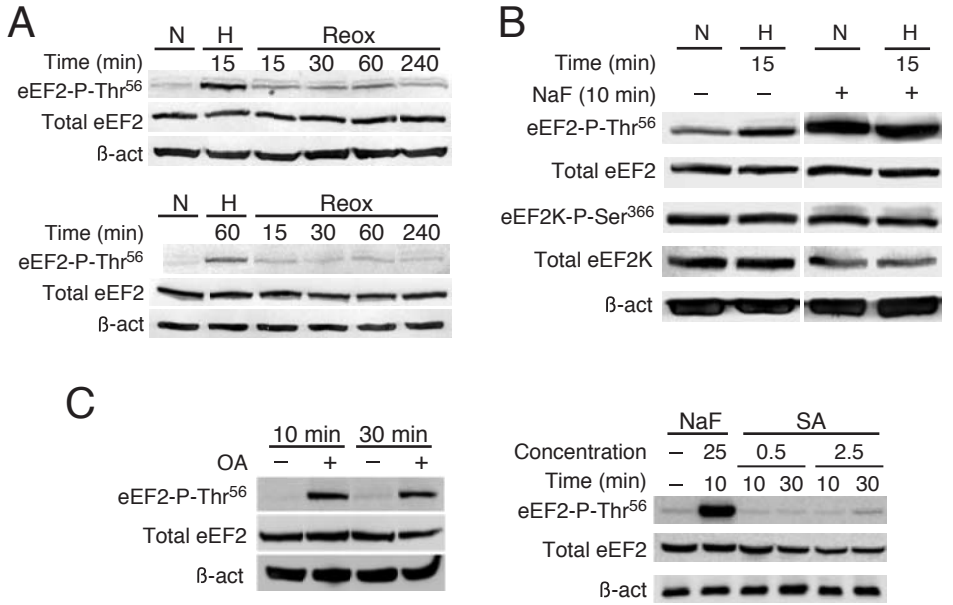

Romero-Ruiz *et al*. Figure 5

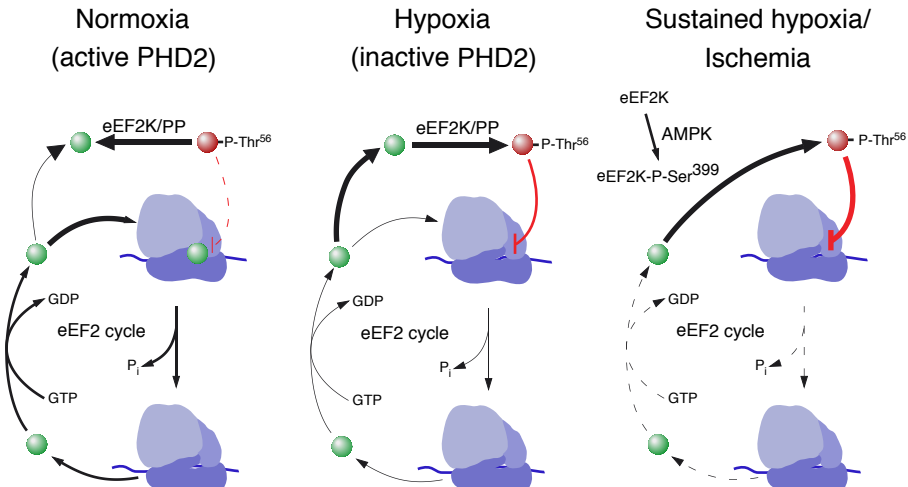

Romero-Ruiz *et al*. Figure 6

Prolyl hydroxylase-dependent modulation of eukaryotic elongation factor 2 activity and protein translation in acute hypoxia

Antonio Romero-Ruiz, Lucía Bautista, Virginia Navarro, Antonio Heras-Garvín, Rosana March-Díaz, Antonio Castellano, Raquel Gómez-Díaz, María J. Castro, Edurne Berra, José López-Barneo and Alberto Pascual

Supplemental data

Supplemental methods

Western blotting. Cells were homogenized in Laemmli sample buffer. Protein concentrations were determined by the RC-DC method (Biorad). Lysates (25-50 μg) were resolved on 8% SDS-polyacrylamide gel electrophoresis followed by transfer to Protein Blotting polyvinylidene difluoride membranes (GE Healthcare). Membranes were probed with the different antibodies (see below) and developed with ECL plus Western blotting detection system (GE Healthcare). Antibodies and dilutions used are: eEF2, Phospho-eEF2 (Thr^{56}), eEF2K, and Phospho-eEF2K (Ser^{366}) (1:1,000; Cell Signaling); AMPK (1/500; Upstate) and AMPK-P-Thr^{172} (1/1,000; Cell Signaling); HIF-1α (1:500; Cayman) (1); HIF-2α (1:1,000; Abcam); and β-actin (1:5,000; Abcam).

Quantification of protein synthesis. Cardiomyocytes were exposed to normoxia, hypoxia (1%) or DMOG (1 mM) for 4 h in serum-free medium. Cells were exposed to Met-free DMEM media supplemented with 0.68 mCi/ml ^{35}S-Met and incubated for additional 15 min under the same conditions. Then, the cells were washed in cold PBS and lysed in RIPA buffer containing complete protease inhibitor cocktel (SIGMA). Proteins were precipitated using TCA. ^{35}S-Met incorporation was measured using a Malisa Star Liquid Scintillation Counter. The amount of radioactivity incorporated was normalized to the protein content of each sample.

Mass spectrometry analysis. MALDI Peptide mass fingerprint and LIFT TOF/TOF spectra were measured on a 4800 plus MALDI TOF/TOF Analyzer (Applied Biosystems). Mass measurements were performed in positive ion reflector mode using 140 ns delayed extraction and a nitrogen laser (337 nm). The laser repetition rate was 50 Hz and the ion acceleration voltage was 25 kV. Mass measurements were performed automatically through fuzzy logic based software to accumulate 100 single laser shot spectra or manually to accumulate 200 single laser shot spectra. Each spectrum was internally calibrated with the mass signals of three trypsin autolysis ions: [VATVSLPR+H]+ (m/z = 842.510), [LSSPATLNSR]+ (m/z = 1045.564) and [LGEHNIDVLEGNEQFINAAK+H]+ (m/z = 2211.105) to reach a typical mass measurement accuracy of ± 20 ppm. Known trypsin and keratin mass signals, as well as potential sodium adducts (+21.982 Da) or signals arising from methionine oxidation (+15.995 Da) were removed from the peak list. The measured tryptic peptide masses exported from the Applied Biosystems 4000 Series Explorer Software v3.5.3 were transferred through Global Proteome Server workstation (v3.0 Applied-Biosystems) as inputs to search the NCBInr database (2008. 06. 28; 6655203 sequences; 2281585098 residues) using Mascot Software (v1.9, Matrix Science). Search default parameters were as follow:

cystein complete carbamidomethylation, methionine partial oxidation, 100 ppm maximal peptide tolerance, and 1 maximal protease missed cleavage. Database search was restricted to mammal sequences. The acceptance criteria was a Mascot score bigger that 71. This score indicates a $p < 0.05$. MS/MS analysis was performed by default with the three ions with the highest abundance in the digested sample. The mass tolerance for fragment ions was 0.2 Da and the cut-off score value for accepting individual MS/MS spectra was a total ion score above 30 in combination with a confidence index above 98.6 %. MS/MS data from LIFT TOF/TOF spectra were combined with MS peptide mass fingerprint data for database searching using Global Proteome Server workstation. The acceptance criteria was the Mascot $p < 0.05$ threshold (Mascot score above 76). All the MALDI-MS spectra obtained are shown in the supporting information. Analysis was performed at SCAI facilities of "Universidad de Cordoba" (Spanish proteomic network, "Proteored").

siRNA and oligonucleotide sequences.

Rat siRNAs:

siRNA control: 5'-CCCUACAUCCCGAUCGAUGdTdT-3'

siRNA PHD1: 5'- UCAGAACUGGGAUGUUAAGdTdT-3'

siRNA PHD2: 5'- GGUGAGCGGAGGUAUUCUUdTdT-3'

siRNA PHD3: 5'- GCAGGAAUCCACAUGAAGUdTdT-3'

Oligonucleotides used in qRT-PCR

PHD1

Human, Mouse, and Rat PHD1 (hPHD1.2; 65bp)

Forward: 5'-TGACCGGTTGCTCATTTTCTG-3'

Reverse: 5'-TGGCATAGGCTGGCTTCAC-3'

PHD2

Human, Mouse, and Rat PHD2 (mPHD2; 68 bp)

Forward: 5'-AGCTGGTCAGCCAGAAGAGT-3'

Reverse: 5'-GCCCTCGATCCAGGTGATCT-3'

PHD3

Human PHD3 (hPHD3.2; 70 bp)

Forward: 5'-GGCTGGGCAAATACTACGTCAA-3'

Reverse: 5'-CCTGTTCCATTTCCCGGATAG-3'

Mouse and Rat PHD3 (mPHD3; 66 bp)

Forward: 5'-CAGACCGCAGGAATCCACAT-3'

Reverse: 5'-CATCGAAGTACCAGACAGTCATAGC-3'

HOUSE-KEEPING

Human 36B4 (Rplp02h; 69 bp)

Forward: 5'-CAGATTGGCTACCCAACTGTT-3'

Reverse: 5'-GGCCAGGACTCGTTTGTACC-3'

Mouse and Rat 36B4 (Arbp01m; 50 bp)

Forward: 5'-TCCAGGCTTTGGGCATCA-3'

Reverse: 5'-CTTTATCAGCTGCACATCACTCAGA-3'

Supplemental figures:

SFig. 1. A. Cardiomyocytes (left), PC12 (middle), and Mlp29 (right) cell lines were subjected to hypoxia (H: 1% O2) for 0-240 min, and phosphorylation at Thr^{56} of eEF2 was examined. The levels of HIF-1α were analyzed in the cardiomyocytes extracts. B. Phosphorylation of eEF2 (Thr^{56}) in HeLa cells subjected to normoxia (N), hypoxia (H: 1% O_2) or DMOG (1 mM) for 0-240 min. Levels of HIF-1α and 2α were analyzed in the same cell extracts. Total level of eEF2 and ß-actin were also analyzed by Western blot.

SFig. 2. A, left. Phosphorylation of eEF2 (Thr^{56}) and levels of HIF-1α examined by Western blot 48 h after siRNA transfection. HuH7 cells were transfected with either PHD siRNAs or with a non-silencing scramble siRNA (Control). Control cells were independently subjected to hypoxia (H) for 15 min. In all the experiments, sample loading was normalized with total eEF2 and ß-actin. A, right. PC12 cells were transfected with siRNAs targeting the three PHDs, or with two different non-silencing control siRNAs (Control 1 and 2). Control cells were independently subjected to hypoxia (H) for 15 min. The eEF2 phosphorylation at Thr^{56} and total levels of eEF2 were examined by Western blot 24 h after transfection. B. Wild-type (*HIF-1α*$^{+/+}$: left) or HIF-1α deficient (*HIF-1α*$^{-/-}$: right) mouse ES cells were exposed to DMOG (1 mM) or hypoxia (Hyp: 1% O2) for 0 to 240 min. Levels of eEF2-P-Thr^{56}, eEF2, HIF-1α, and ß-act were examined by Western blot.

Supplemental Table I:

Spots modified by hypoxia and DMOG treatments.

			15 min Hypoxia		30 min Hypoxia		15 min DMOG		
ID[1]	Protein accession Number	Protein Name (Gen name)	*p* value	Fold change[2]	*p* value	Fold change[2]	*p* value	Fold change[2]	M.S.[3]
1	NP_058941	Eukaryotic translation elongation factor 2 (*eEF2*)	0.01400	1.51	0.03950	1.62	0.0129	1.66	312
2			0.03860	1.76	0.01050	2.03	n.s.c.[4]	n.s.c.	
3			0.01842	1.51	0.00312	1.75	n.s.c.	n.s.c.	
4			0.00710	1.56	0.00043	1.79	n.s.c.	n.s.c.	
5			0.02961	1.61	0.00410	2.16	n.s.c.	n.s.c.	
6			0.01241	1.72	0.00422	1.96	n.s.c.	n.s.c.	
7			0.03458	1.65	0.01777	1.80	n.s.c.	n.s.c.	
8			0.00168	1.61	0.02707	2.30	n.s.c.	n.s.c.	
9			0.02834	1.52	0.00244	1.75	n.s.c.	n.s.c.	
10			0.02483	1.56	0.01844	1.62	n.s.c.	n.s.c.	
11			0.00470	1.52	0.00379	1.51	n.s.c.	n.s.c.	
12			0.00415	1.55	0.02765	1.54	n.s.c.	n.s.c.	
13	NP_112359	Arginyl aminopeptidase (*Rnpep*)	0.01183	1.70	0.00819	1.74	n.s.c.	n.s.c.	513
14			0.00750	-1.61	0.00265	-1.71	n.s.c.	n.s.c.	
15			0.01729	1.52	0.01383	1.51	n.s.c.	n.s.c.	
16			0.00634	1.84	0.00111	2.44	n.s.c.	n.s.c.	
17			0.00940	1.64	0.00987	1.75	n.s.c.	n.s.c.	
18			0.00806	-1.52	0.00747	-1.55	n.s.c.	n.s.c.	
19	NP_954516	Serine peptidase inhibitor; clade B; member 6a (*Serpinb6a*)	0.00074	1.58	0.00019	1.59	n.s.c.	n.s.c.	197
20			0.00011	1.51	0.01903	1.73	n.s.c.	n.s.c.	
21	NP_001014139	Ubiquitin-like domain containing CTD phosphatase 1 (*Ublcp1*)	0.00149	1.61	0.00057	1.68	n.s.c.	n.s.c.	68
22			0.01073	1.58	0.00008	1.86	n.s.c.	n.s.c.	
23			0.00401	-1.52	0.00516	-1.59	n.s.c.	n.s.c.	
24			0.01140	-2.96	0.02500	-3.01	n.s.c.	n.s.c.	

1. ID numbers correspond to spots encircled in Fig. 1; 2. Positive values applies to spots with increased levels in hypoxia or DMOG, negative ones to relative amounts increased in Normoxia; 3. M.S.: Mascot Score; 4. n.s.c.: No significant change.

Arginyl aminopeptidase removes arginine and/or lysine residues from the amino terminal end of proteins (2) and is required for neuropeptides maturation, including enkephalin, a well-known vasodilator of cerebral arteries (3, 4). This enzyme seems to be implicated in inflammatory responses and tumor progression (5). The protease inhibitor Serpinb6 has also been related with inflammation and protection against cerebral ischemia (6). Nonetheless, whether Serpinb6 and arginyl aminopeptidase play any relevant role in O2 homeostasis is a question not addressed in the current study and left for future experimental work.

Supplemental Table II. Efficiency of siRNA treatments.

PC12 silencing of PHDs with siPHD1+2+3

SIMA	100
PHD1 (siPHDs)	38.85
PHD2 (siPHDs)	30.17
PHD3 (siPHDs)	33.77

HeLa silencing of HIF/PHDs

SIMA	100
HIF1 (siHIFs)	4.18
EPAS (siHIFs)	4.14
PHD1 (siPHD1)	36.78
PHD1 (siPHDs)	22.98
PHD2 (siPHD2)	24.38
PHD2 (siPHDs)	32.06
PHD3 (siPHD3)	13.87
PHD3 (siPHDs)	29.26

Supplemental references:

1. Ginouves A, Ilc K, Macias N, Pouyssegur J, Berra E (2008) PHDs overactivation during chronic hypoxia "desensitizes" HIFalpha and protects cells from necrosis. *Proc Natl Acad Sci U S A* 105:4745-4750.
2. Foulon T, Cadel S, Cohen P (1999) Aminopeptidase B (EC 3.4.11.6). *Int J Biochem Cell Biol* 31:747-750.
3. Balogh A*, et al.* (1998) Aminopeptidase B: a processing enzyme secreted and associated with the plasma membrane of rat pheochromocytoma (PC12) cells. *J Cell Sci* 111:161-169.
4. Benyo Z, Wahl M (1996) Opiate receptor-mediated mechanisms in the regulation of cerebral blood flow. *Cerebrovasc Brain Metab Rev* 8:326-357.
5. Piesse C*, et al.* (2002) Human aminopeptidase B (rnpep) on chromosome 1q32.2: complementary DNA, genomic structure and expression. *Gene* 292:129-140.
6. Nakaya N, Nishibori M, Wang Z, Sakiyama J, Saeki K (1998) The expression and localization of serine proteinase inhibitor PI-6 mRNA in developmental and ischemic mouse brain. *Neurosci Res* 32:221-230.

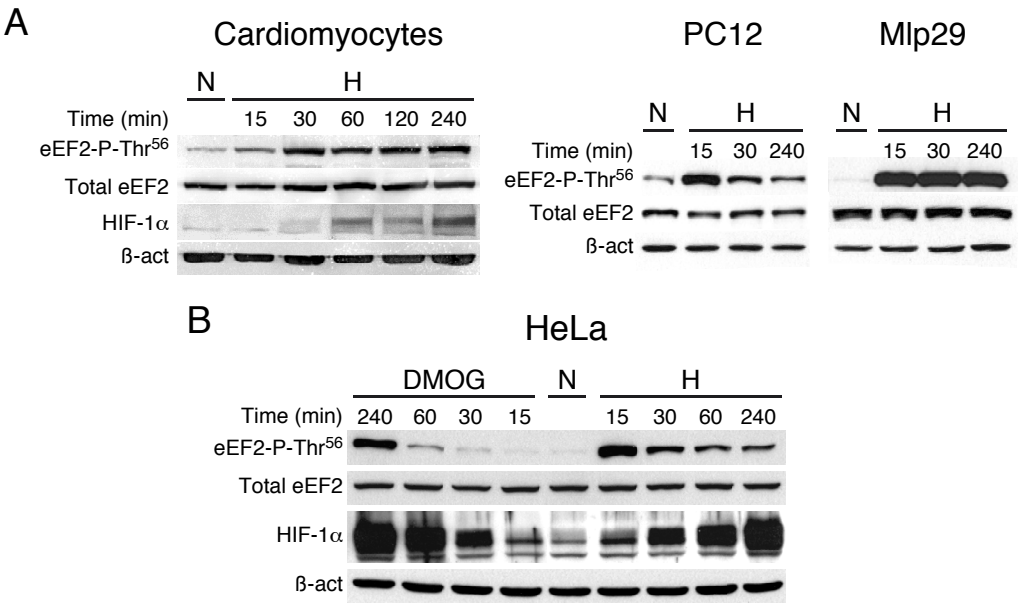

Romero-Ruiz *et al*. SFig. 1

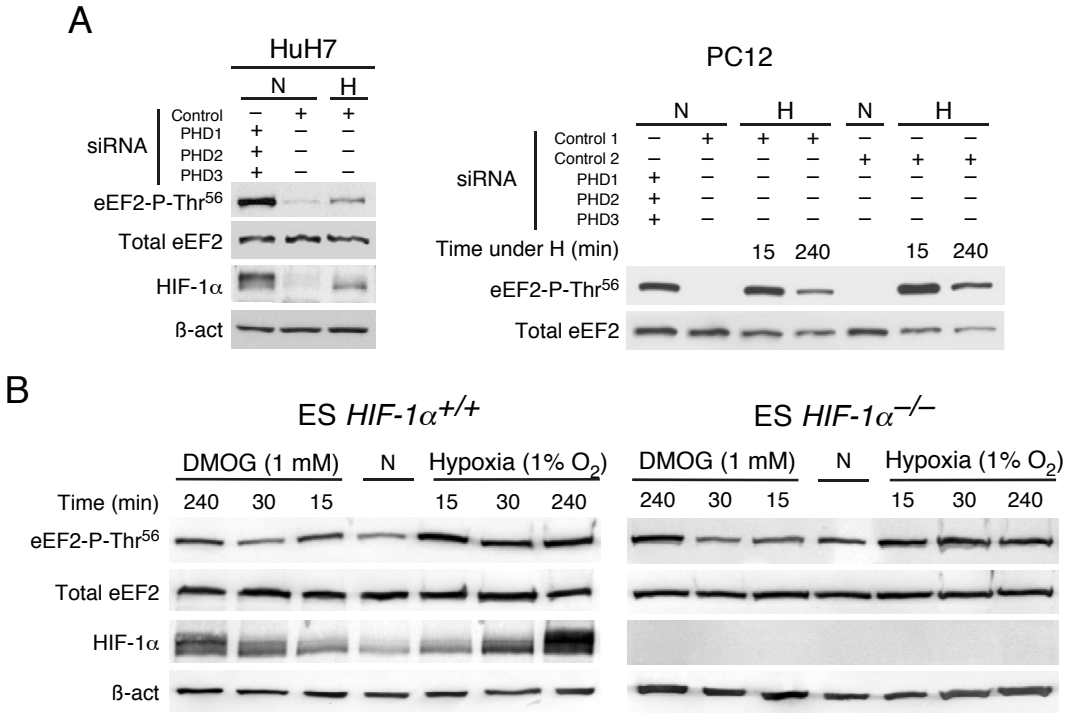

Romero-Ruiz *et al*. SFig. 2